

Microseisms: Mode Structure and Sources

Abstract. Frequency-wave number spectra of microseisms were obtained by use of a set of short-period and long-period seismometers at LASA (Large Aperture Seismic Array, Montana). At times of relatively high microseismic activity short-period (shorter than 5 seconds) microseisms consist of both body waves and higher-mode surface waves. From the phase velocity and direction of body waves, source areas were determined, coinciding with low-pressure regions on the weather map. At longer periods, microseisms consist of fundamental-mode Rayleigh and Love waves, the former being dominant. Most microseismic energy arrives at LASA from the northeast and the west.

Continuous vibrations of the ground, called microseisms, have been a classic subject of study for earth scientists (1). Various aspects of the microseismic noise—its source (2), modes of generation (3), propagation, utilization for practical purposes (4), and elimination in seismic-signal processing (5)—have been investigated. Earlier studies, concerned primarily with waves with periods greater than about 3 to 4 seconds, used single stations or tripartite arrays. More recently short-period horizontal and vertical seismic arrays of limited spatial extent have been used for study of microseisms; it was found that at short periods microseismic waves may contain some higher-mode Rayleigh waves and some body waves (6), but the small apertures of such arrays limited results to relatively short wavelengths.

We have investigated microseisms, of both short and long periods, using the Large Aperture Seismic Array (LASA) in Montana. The array consists of 525

short-period vertical and 21 three-component long-period seismometers distributed over an area about 200 km in diameter (7). It provides the desired large aperture and seismometer density for wave-number resolution over a very broad range of frequency.

We consider microseisms as a random process, stationary in time and space over time intervals equal to the sample lengths. In essence we then compute the three-dimensional Fourier transform of the correlation function of space and time variables. The result gives power spectral density in frequency-wave number space: that is, the power at each frequency as a function of phase velocity and direction of approach. The mathematical formulations and the techniques used will be reported separately (8).

For investigation of short-period (shorter than 5 seconds) microseisms we used sets of 28 and 36 vertical short-period seismometers for forming

beams; these sets were chosen to provide a fairly uniform spatial coverage. Microseism records 6 to 12 minutes in duration were analyzed on different days. The results for a typical day are shown (Fig. 1) as plots of the power level (relative to peak power) at each frequency as a function of east and north components of the wave number; the origin corresponds to zero wave number or infinite phase velocity. At a given frequency f , the increasing wave number k means a lower phase velocity c , since these quantities are related by $c = f/k$. At $f = 0.2$ hz (Fig. 1) we see power peak in the northeast quadrant. Such a peak corresponds to a direction of approach of microseisms to LASA from about N50°E with a phase velocity of about 3.5 km/sec. At $f = 0.3$ hz, in addition to the previous peak, an arrival from the west, having much greater phase velocity (13.5 km/sec), becomes apparent. At higher frequencies (0.4 or 0.6 hz) the low-velocity peak disappears and the two well-defined high-velocity peaks become prominent.

Seismic waves having such high phase velocities (13.5 km/sec) correspond to compressional body waves, and we may conclude that, for this particular example, the high-frequency microseisms recorded at LASA consist predominantly of seismic P waves. The peak at $f = 0.2$ hz and $c = 3.5$ km/sec corresponds to first or second higher Rayleigh mode. The Rayleigh-wave dispersion curves for a preliminary LASA structure appear in Fig. 2.

Analyses of short-period microseism data recorded on other days show similar results. As an example we have summarized all arrivals from westerly directions (Fig. 3a); each point corresponds to a peak in the frequency-wave number diagrams such as Fig. 1. From the grouping of the data, clearly we can identify two modes of propagation: (i) the high-velocity body waves and (ii) the low-velocity surface waves. Figure 2 shows that the surface waves again correspond to higher Rayleigh modes rather than the fundamental mode. Microseismic arrivals from the east give results almost identical with those from the west.

At long periods, microseisms were analyzed by similar techniques with longer time samples and a subset of the 21 three-component seismometers. The frequency-wave number results for the vertical components of the motion are summarized in Fig. 3b; the dispersion curve corresponds to that of a funda-

Table 1. Cross spectra of microseisms on 29 December 1966 (azimuth, 298°; c , 3.7 km/sec; f , 0.065 hz). i , Indeterminate number.

	$Z(i)$	$R(i)$	$T(i)$
Z (Vertical)	1025 + 0	39 - 948	-214 - 76
R (Radial)	39 + 948	984 + 0	151 - 183
T (Transverse)	-214 + 76	151 + 183	2174 + 0

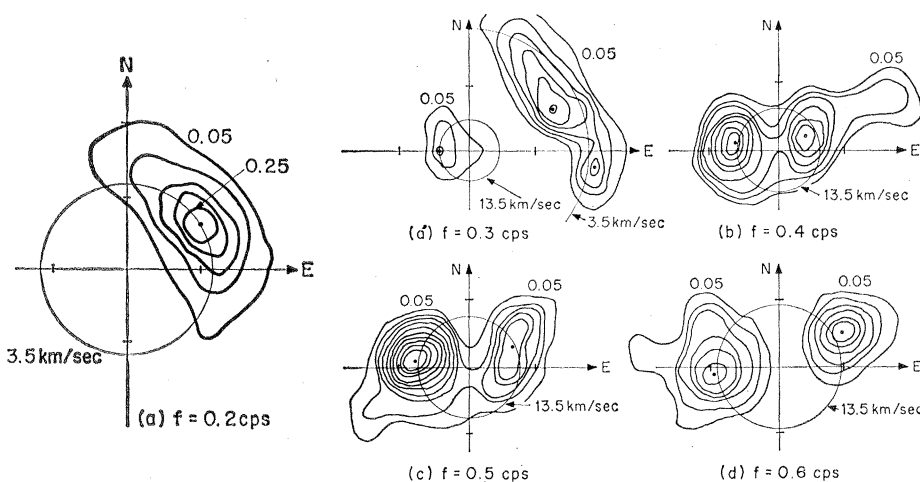


Fig. 1. Wave-number structure of microseisms on 2 December 1965. Coordinate axis is graduated in units of 0.05 cy/km.

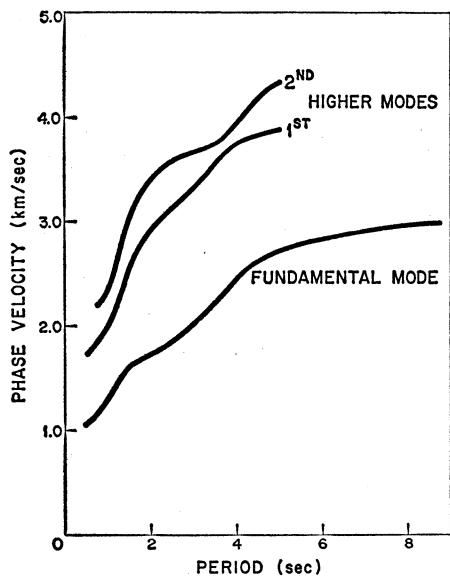


Fig. 2. Theoretical Rayleigh-wave dispersion curves for an average structure of LASA.

mental-mode Rayleigh wave. Thus we can conclude that at periods longer than about 6 seconds the vertical component of microseismic motion is due to fundamental-mode Rayleigh waves.

The presence of Love waves in long-period microseisms is also observed for one of the microseismic peaks. After the main source of energy was determined, a beam was formed; the horizontal seismometer outputs were combined to form purely radial and

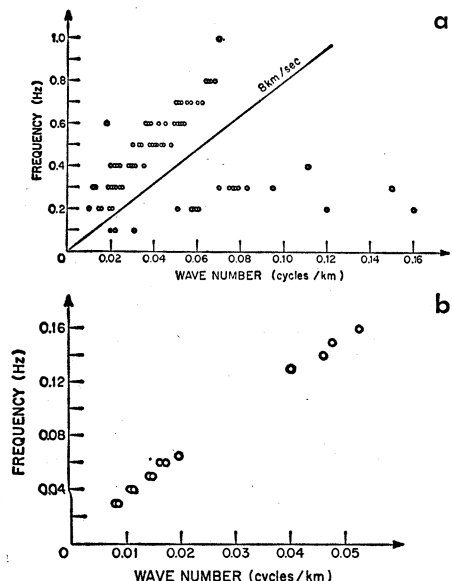


Fig. 3. (a) Cumulative frequency-wave number plot of microseism power peaks arriving from the west. Note the separation of surface waves and body waves on two sides of 8-km/sec line. (b) Frequency-wave number dispersion curve for the long-period vertical motion of microseisms; it corresponds to fundamental-mode Rayleigh-wave dispersion.

transverse components of the motion. The elements of the cross-spectral matrix at $f = 0.065$ hz are listed (Table 1), showing that the vertical and radial motions are approximately equal and highly correlated with a phase difference of 90 deg; this finding corresponds to retrograde Rayleigh motion and hence to fundamental Rayleigh mode. The transverse component, larger than the radial by a factor of 2, does not correlate with the radial or the vertical motion; it corresponds to a Love wave coming from the same direction as the Rayleigh wave. Since there were no other prominent peaks in the frequency-wave number diagram for that time, this transverse motion cannot be due to Rayleigh waves arriving from a different direction.

Let us now summarize the results: On a typical day the microseisms recorded in Montana consist of both body waves and multi-mode surface waves. At frequencies higher than 0.3 hz most of the microseisms consist of compressional body waves. In the frequency range between 0.2 and 0.3 hz both body waves and higher-mode Rayleigh waves are observed, with the relative power of surface waves increasing with decrease in frequency. At frequencies below 0.15 hz the microseisms consist primarily of fundamental-mode Rayleigh waves; appreciable amounts of fundamental-mode Love-wave energy also may be present. These results constitute very comprehensive data about the mode structure and the composition of the microseisms; they cover a very broad frequency range from 0.04 to 0.6 hz, and provide greater resolution than earlier results.

We must emphasize that these results apply to LASA and probably to the interiors of other continents. In coastal regions and near great lakes, fundamental-mode Rayleigh waves may be present even at higher frequencies, provided that these can be generated nearby. We do not expect short-period surface waves to propagate over great distances from source regions, since such waves attenuate rapidly because of crustal inhomogeneities and surface irregularities.

Frequency-wave number diagrams such as Fig. 1 enable us to determine directly the source of the body-wave component of a microseism; they provide the direction and the phase velocity of the body wave, and the source region can be determined from the projected ray paths. In this instance the sources are in the Labrador Sea, centered at about $50^{\circ}\text{N}, 43^{\circ}\text{W}$, and in the Pacific

Ocean at $35^{\circ}\text{N}, 160^{\circ}\text{W}$. These areas correspond to stationary low-pressure regions on the weather map for the same day and two previous days; thus we can conclude that the body waves in microseisms are due to the atmosphere-ocean interaction and the resultant pressure fluctuations at the bottom of the ocean; such fluctuations have been observed with ocean-bottom instruments (9). By correlation of weather maps, ocean waves, and microseisms, other studies have shown that the source of a low-frequency microseism is also the coupling of energy between water bodies, such as oceans, and Earth's crust (3, 9).

The Love waves cannot be excited by pressure fluctuations at the bottom of the ocean. They must be due to either the conversion of Rayleigh waves to Love waves along complicated propagation paths, or surf action or other motions where shear forces are exerted on the solid medium.

The contribution (if any) by very small earthquakes, creep action, or other dislocations in Earth's crust to the observed microseisms seems to be very small. In our frequency-wave number studies we could not find power peaks pointing in the directions of Earth's seismically active regions.

M. NAFI TOKSÖZ

RICHARD T. LACOSS

Department of Geology and Geophysics, and Lincoln Laboratory, Massachusetts Institute of Technology, Cambridge

References and Notes

1. B. Gutenberg, *Advances in Geophysics* (Academic Press, New York, 1958), vol. 5, p. 53; E. Hjortenberg, *Mem. Geodæt. Inst. Denmark Ser. 3* 1967, 38 (1967).
2. R. A. Haubrich, W. H. Munk, F. E. Snodgrass, *Bull. Seism. Soc. Amer.* 53, 27 (1963); J. Oliver and R. Page, *ibid.*, p. 15; H. Bradner, J. C. Dodds, R. Foulks, *Geophysics* 30, 511 (1965); E. J. Douze, *Bull. Seism. Soc. Amer.* 57, 55 (1967).
3. M. S. Longuet-Higgins, *Phil. Trans. Roy. Soc. London Ser. A* 243, 1 (1950); K. Hasselman, *Rev. Geophys.* 1, 177 (1963).
4. M. N. Toksöz, *Geophysics* 29, 154 (1964); K. Aki, *ibid.* 30, 665 (1965).
5. M. M. Backus, J. P. Burg, R. Baldwin, E. Bryan, *ibid.* 29, 672 (1964).
6. R. L. Sax and R. A. Hartenberger, *ibid.*, p. 714; A. J. Seriff, C. J. Velzeboer, R. J. Haase, *ibid.* 30, 1187 (1965); R. A. Haubrich, *J. Geophys. Res.* 70, 1415 (1965).
7. P. E. Green, Jr., R. A. Frosch, C. F. Romney, *Proc. Inst. Elec. Electron. Engrs.* 1965, 1821 (1965).
8. R. T. Lacos, E. J. Kelly, M. N. Toksöz, in preparation.
9. H. Bradner and J. C. Dodds, *J. Geophys. Res.* 69, 4339 (1964); W. A. Schneider and M. Backus, *ibid.*, p. 1134; G. V. Latham and J. H. Sutton, *ibid.* 71, 2545 (1966).
10. Aided by the Advanced Research Projects Agency and monitored by the Air Force Office of Scientific Research under contract AF 49 (638)-1632. Lincoln Laboratory is assisted by ARPA. We thank E. J. Kelly for suggestions and D. G. Harkrider for assistance in dispersion calculations.

24 November 1967